sustainability

MDPI

Article

Study on Occurrence Mechanism and Prevention Technology of Rock Burst in Narrow Coal Pillar Working Face under Large Mining Depth

Shitan Gu [1], Huaixu Chen [1], Wenshuai Li [2,*], Bangyou Jiang [1,*] and Xiang Chen [3]

[1] College of Energy and Mining Engineering, Shandong University of Science and Technology, Qingdao 266590, China
[2] Shandong Key Laboratory of Civil Engineering Disaster Prevention and Mitigation, Shandong University of Science and Technology, Qingdao 266590, China
[3] Shandong Jining Yunhe Coal Mine Co., Ltd., Jining 272000, China
* Correspondence: wenshuai_li@sdust.edu.cn (W.L.); jiangbangyou123@163.com (B.J.)

Abstract: This paper presents a collaborative control scheme involving "unloading-solidifying" to prevent rock bursts during narrow pillar recovery at large mining depths. In this study, the stress distribution rule of coal rock mass during the excavation and mining process is studied, and the energy accumulation characteristics of the overlying hard and thick roof structure are investigated. In this way, the rock burst inducing mechanism of the narrow coal pillar working face under complex conditions is investigated. The results show that the peak lateral bearing pressure of the goaf and the maximum horizontal principal stress provide the static load condition for the occurrence of rock burst during roadway excavation. Affected by the superposition of "near-field high static load + far-field dynamic load", it is extremely easy to reach the critical destabilization value during the mining period at the narrow coal pillar working face. According to the monitoring results, the developed coordinated control scheme, which focuses on the strong pressure relief and strong support in near-field high-bearing pressure coal mass and the pressure relief in far-field high-level hard roof with an advanced pre-cracking roof, can effectively avoid the occurrence of rock burst accidents on narrow coal pillar working face.

Keywords: narrow coal pillar; rock burst; rock burst inducing mechanism; hard roof; prevention and control

Citation: Gu, S.; Chen, H.; Li, W.; Jiang, B.; Chen, X. Study on Occurrence Mechanism and Prevention Technology of Rock Burst in Narrow Coal Pillar Working Face under Large Mining Depth. *Sustainability* **2022**, *14*, 15435. https://doi.org/10.3390/su142215435

Academic Editors: Kai Wang, Yubing Liu and Xiaojun Feng

Received: 4 October 2022
Accepted: 16 November 2022
Published: 20 November 2022

1. Introduction

Coal has been the primary source of energy on which the development of many countries depends. With the rapid development of China's economy, the status of coal as a main energy source will not change for quite a long time [1–3]. However, the coal mining environment in China is complicated and affected by geological conditions, mining conditions, and other factors. It is often accompanied by a variety of mine disaster accidents. Among them, the rock burst represents a common coal mine dynamic disaster. A rock burst releases the coal rock mass' deformation energy in a sudden, rapid, and violent manner and throws out the coal rock mass, resulting in support damage, roof fall, rib spalling and casualties, and severely restricts the production and development of the mine [4–7]. On the other hand, with increasing economic and social development, long-term and high-intensity resource exploitation is making a large number of mines in eastern China enter the recession period of resource development [8]. With the exhaustion of mining resources in eastern mines, a large number of side and corner coal pillars will be recovered later, with some having narrow working faces. However, during recovery of side and corner coal pillars, influenced by the hard roof, working face width, etc., the possibility of transitioning from conventional mine pressure behavior to rock burst disasters increases. Furthermore,

the weighting on working face is strong, which complicates the prediction and prevention of rock bursts. Therefore, it is of great engineering significance to study the occurrence mechanism and prevention method of rock bursts under such working conditions.

Numerous academics have been conducting relevant research and exploration into the mechanism of rock burst as well as its prevention and control [9–13]. Xu et al., [14] analyzed the destructive characteristics and disaster-causing factors of a large number of rock burst roadways in China, and put forward the strategies for prevention and control of rock burst. Zhao et al., [15] observed and examined the spatio-temporal and geological aspects of rock burst occurrence in Muchengjian Coal Mine. Additionally, many scholars have carried out research on the rock burst inducing mechanism for hard roof [16–19], fault [20–24], etc., providing helpful guidance for the prevention and control of rock burst.

Researchers have also studied the mechanism that causes rock burst, as well as ways to prevent and manage them under unique or challenging work conditions. Jiang et al., [25] studied the destabilization mechanism of an isolated island working face in combination with dynamic change process of irregular goaf structure on both sides of the coal pillar working face. Xue et al., [26] studied the rock burst mechanism in a deep irregular isolated island coal pillar area and formulated a pressure relief scheme under dynamic and static load. Du et al., [27] simulated and analyzed the stress distribution rule of coal rock mass with different structural forms in the context of goaf roadway beneath the residual coal seam of hard roof. Zhu et al., [28] assessed the burst risk of an isolated island working face based on the spatial structure theory of overlying strata. The above-mentioned studies are of great significance for understanding the occurrence mechanism of rock burst under complex conditions and guiding the prevention and control of rock bursts at the working face.

However, the above studies mainly focused on the occurrence mechanism for rock bursts at the working face under some special conditions. The occurrence mechanism, as well as prevention and control methods of rock burst at narrow coal pillar working face under complex conditions (including goafs around the working face, large burial depth, hard roof and narrow inclined length) still need to be further explored. In this paper, with the typical narrow working face of a mine as the technical background, the energy accumulation mechanism and breaking energy of hard roof during mining are investigated. Additionally, the occurrence mechanism of rock bursts is explored, and the corresponding prevention and control scheme of rock bursts is formulated.

2. Engineering Background

In the present study, the 3# coal seam has been taken as the reference for the investigation. It is 7.35–7.55 m thick and has a dip angle of 2–13°, with complex geological conditions. The 6304 working face is a typical narrow coal pillar working face, with a burial depth of 636–797 m and an inclined length of 40 m. On the north side of this working face is a mine-out area (6302 goaf), and there is a 5 m coal pillar between the two working faces. On the south side of the working face is the −725 west wing belt roadway and the southwest side is about 135 m away from the 3312 goaf. Figure 1 shows the arrangement of the working face. The coal mining method of working face is fully mechanized top coal caving, and the goaf is treated by all caving method. According to the actual geological information of the coal mine, the borehole rock structure near the 6304 working face is shown in Table 1 and Figure 2. The roof of 3# coal seam is fine sandstone with a thickness of 15.2 m and an average compressive strength of 97.35 MPa. The roof is not easy to collapse during mining.

According to the crustal stress analysis report of the mine, the maximum principal stress of the original rock stress field is the horizontal stress and the maximum horizontal principal stress is 1.34–1.57 times that of the vertical stress. The maximum principal stress of the YHMK2 measuring point near the 6304 working face is horizontal stress, as shown in Figure 1, and the maximum horizontal stress is approximately perpendicular to the roadway of the 6304 working face.

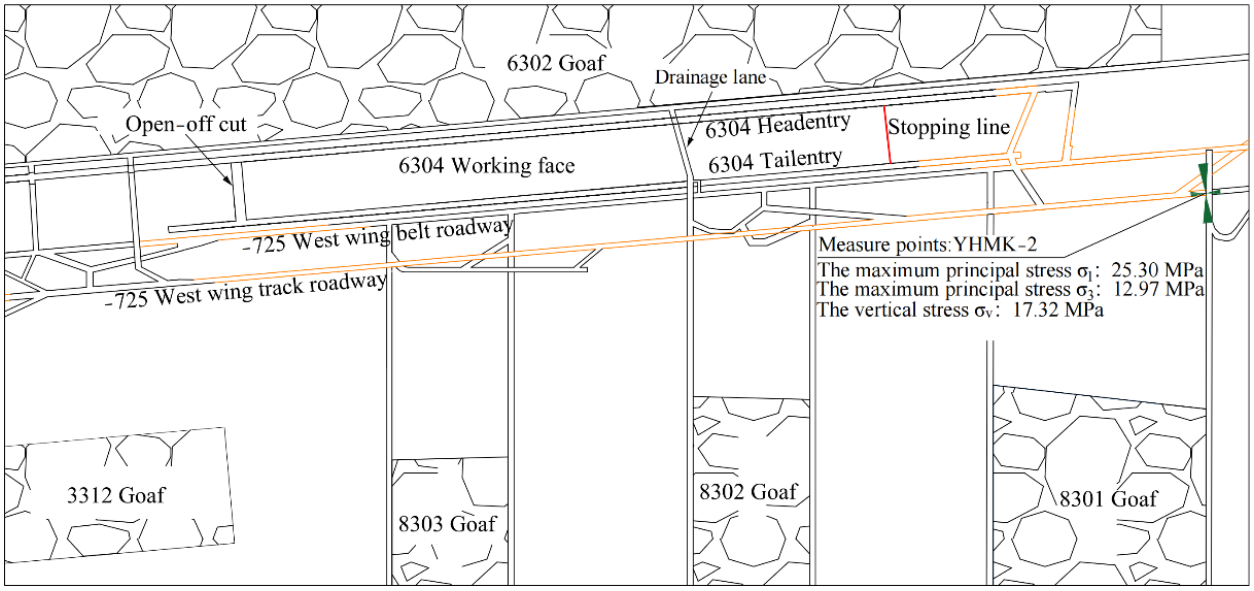

Figure 1. The arrangement of 6304 working face.

Lithological geological column	Thickness (m)	Lithology	Lithology description
	3.20	Fine sandstone	Light gray, silty and mixed with siltstone. It is mainly composed of quartz and feldspar.
	5.90	Siltite	It is gray and contains more fossilized plant fragments and punctate pyrite.
	1.80	Siltite	It is dark gray in color and contains clay and a few plant fragments.
	2.80	Mudstone	It is dark gray in color and contains more fossilized plant roots and siderite nodules.
	0.90	Fine sandstone	Light gray, silty and mixed with siltstone. It is mainly composed of quartz and feldspar.
	1.15	Siltite	It is dark gray in color and contains a thin layer of clay and carbonaceous mudstone.
	0.10	2# Coal	It is black in color with asphalt sheen. The shape is block, uniform and banded structure.
	1.10	Mudstone	It is light gray and rich in fossilized plant roots.
	15.20	Fine sandstone	Light gray, silty and mixed with siltstone. It is mainly composed of quartz and feldspar.
	0.65	Siltite	It is dark gray in color and contains plant fragments fossil and more pyrite nodules and film.
	7.45	3# Coal	It is black with asphalt luster and grease luster. The upper part is dominated by bright coal and the lower part is dominated by dark coal.
	1.85	Mudstone	It is brown gray and contains plant root fossil and pyrite film.

Figure 2. Borehole stratum structure drawing of 6304 working face.

The working face has a higher burst risk during excavation due to a number of factors. During excavation, the amount of coal powder drilled using the drilling cuttings method exceeded the critical value six times. The early warning of microseismic monitoring occurred 22 times, and that of stress online monitoring occurred 7 times. During mining period, the amount of coal powder drilled by the drilling cuttings method surpassed the critical value 4 times. The early warning of microseismic monitoring occurred 30 times, and that of stress online monitoring occurred 24 times. Table 2 and Figure 3 show the monitoring and early warning results. Furthermore, dynamic events frequently occurred during the mining period. The anchor cable tray fell off and the anchor rod broke in parts of the two roadways, as shown in Figure 4.

Table 1. Borehole stratum structure of the 6304 working face.

Rock Number	Lithology	Thickness/m	Rock Number	Lithology	Thickness/m
19	Medium sandstone	7.00	9	Siltite	5.90
18	Mudstone	4.57	8	Siltite	1.80
17	Fine sandstone	7.75	7	Mudstone	2.80
16	Mudstone	4.97	6	Fine sandstone	0.90
15	Fine sandstone	1.80	5	Siltite	1.15
14	Mudstone	6.30	4	2# Coal	0.10
13	Siltite	12.38	3	Mudstone	1.10
12	Fine sandstone	0.80	2	Fine sandstone	15.20
11	Mudstone	2.30	1	Siltite	0.65
10	Fine sandstone	3.20	Coal	3# Coal seam	7.45

Table 2. Overview of monitoring and early warning during excavation and mining of 6304 working face.

Monitoring Methods	During Excavation		During Mining	
	Warning Number	Warning Area	Warning Number	Warning Area
Drilling cuttings method	6	Stop excavation area of tailentry; 21 m ahead of the 10# point of tailentry	4	Point 25# of headentry
Microseismic monitoring	22	Near the former drainage lane area of 6302; between points 12# and 13# of tailentry	30	The 12# point of tailentry; between points 25# and 26# in headentry
Stress online monitoring	7	21 m ahead of the 10# point of tailentry	24	Area in12# and 14# points of tailentry; near the former drainage lane area of 6302

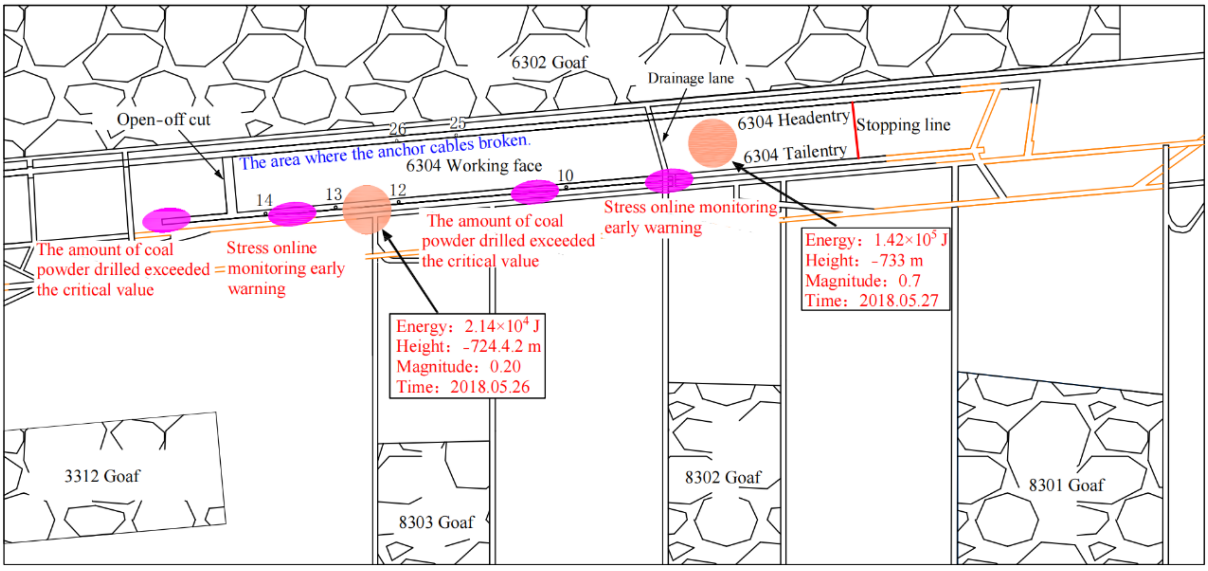

Figure 3. Schematic diagram of early warning during excavation and mining of 6304 working face.

Figure 4. Diagram of field support failure.

3. Occurrence Mechanism of Roadway Rock Burst in Narrow Coal Pillar Working Face

3.1. Energy Accumulation Mechanism of the Coal Seam in Narrow Working Face

To investigate the stress distribution features of coal rock mass during the mining of the narrow working face, the 6304 working face is taken as the study object, to build a Fast Lagrangian Analysis of Continua (FLAC3D) numerical calculation model. The model reflects the actual geological conditions of the working face. The model size (length × width × height) is 480 × 314 × 120 m, as shown in Figure 5. The Mohr-coulomb model is used for calculation. Horizontal displacement constraints are applied around the model; vertical displacement constraints are applied at the bottom; and the equivalent overburden load of 16.6 MPa is applied according to the burial depth. The mechanical parameters of coal and rock for the model are assigned according to the borehole characteristics near the working face and the experimental results of rock mechanics. The mechanical parameters of the coal and rock are listed in Table 3. Excavation scheme. Firstly, the goaf and roadway around 6304 working face are excavated to study the stress distribution of 6304 working face before excavation, and then the working face is excavated to study the distribution characteristics and evolution process of the stress during mining.

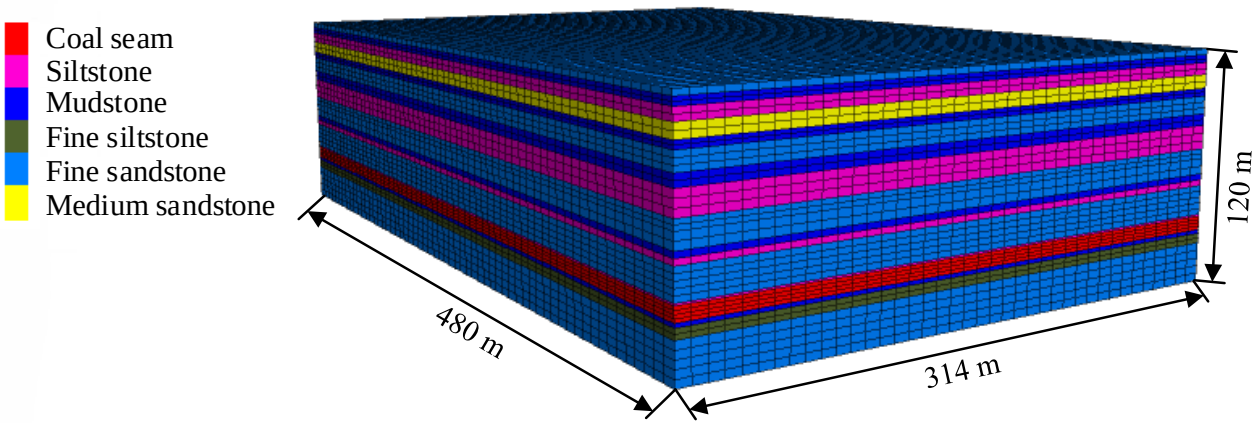

Figure 5. Schematic diagram of the numerical model.

Table 3. Mechanical parameters of coal and rock.

Lithology	Density/kg/m^3	Bulk Modulus/GPa	Shear Modulus/GPa	Strength of Extension/MPa	Cohesion/MPa	Friction Angle/(°)
Coal seam	1500	6.67	1.13	1.5	2.15	27
Fine sandstone	2600	18.44	12.15	3.5	5.8	38
Mudstone	2200	10.85	3.89	2.47	3.1	30
Siltstone	2600	15.44	9.15	3.5	5.8	38
Medium sandstone	2500	18.44	12.15	3.5	5.8	38
Fine siltstone	2500	17.96	12.36	3.8	5.93	37

Figure 6 depicts a cloud diagram showing the stress distribution characteristics of the coal seam in the working face before mining. Figure 7 shows the stress distribution curve of coal pillar in 6304 working face before roadway excavation (measuring line position is shown by the red dashed line in Figure 6). As can be seen in Figure 6, since the 6304 working face is relatively narrow, 6304 working face is in the influence range of lateral bearing pressure of the previous working face after the mining of 6302, 8301, 8302, and 8303 working faces. The stress concentration of 6304 working face near 6302 goaf is relatively high, which is about 40 MPa. During roadway excavation in 6304 working faces, the roadway will be in the affected area of peak lateral bearing pressure of 6302 goaf.

Figure 8 shows a cloud diagram for the distribution of stress on the coal rock mass under various advancing steps. Figure 9 shows a distribution rule for the advanced bearing pressure of the working face under various advancing steps (measuring line is shown by the red dashed line in Figure 8). As mining progresses, the peak value of the advanced bearing pressure at the working face gradually increases, as does the stress concentration near the advanced working face. The peak value of the advanced bearing pressure is generally in the range of 12–15 m at the advanced working face. The peak values of the bearing pressure advanced 50 m, 100 m, 150 m, and 200 m are 61.7 MPa, 78.1 MPa, 88.3 MPa, and 92.3 MPa, respectively (Figure 8). The coal mass experiences high tension as the goaf area expands, making it extremely easy to induce rock bust accidents under high stress.

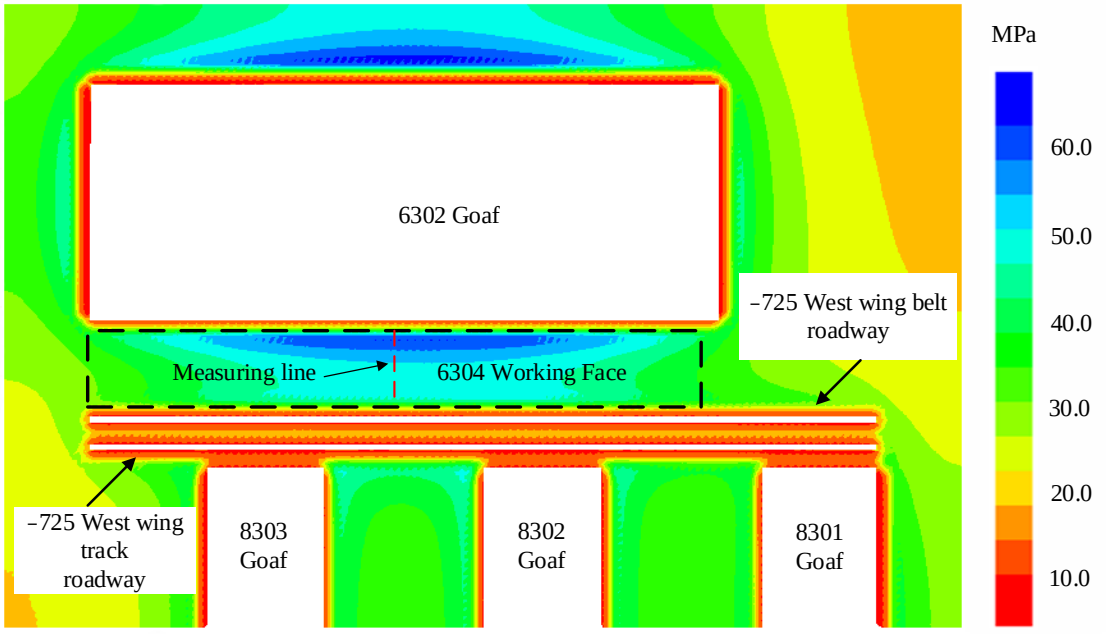

Figure 6. Stress distribution diagram of the working face before mining.

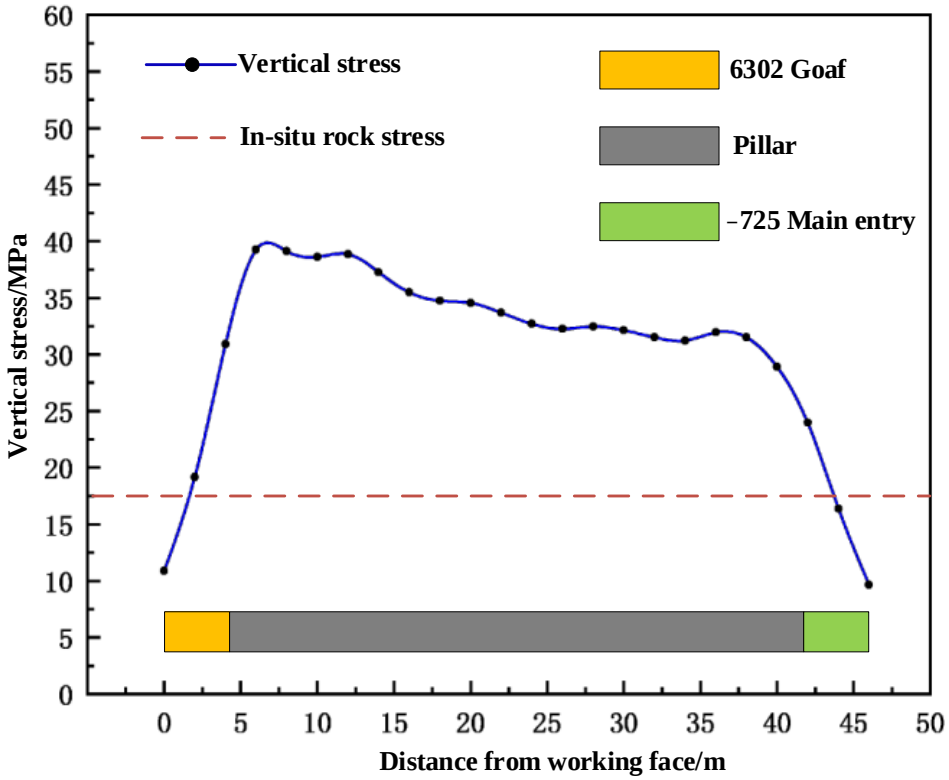

Figure 7. Stress distribution curve of coal pillar in the working face before excavation.

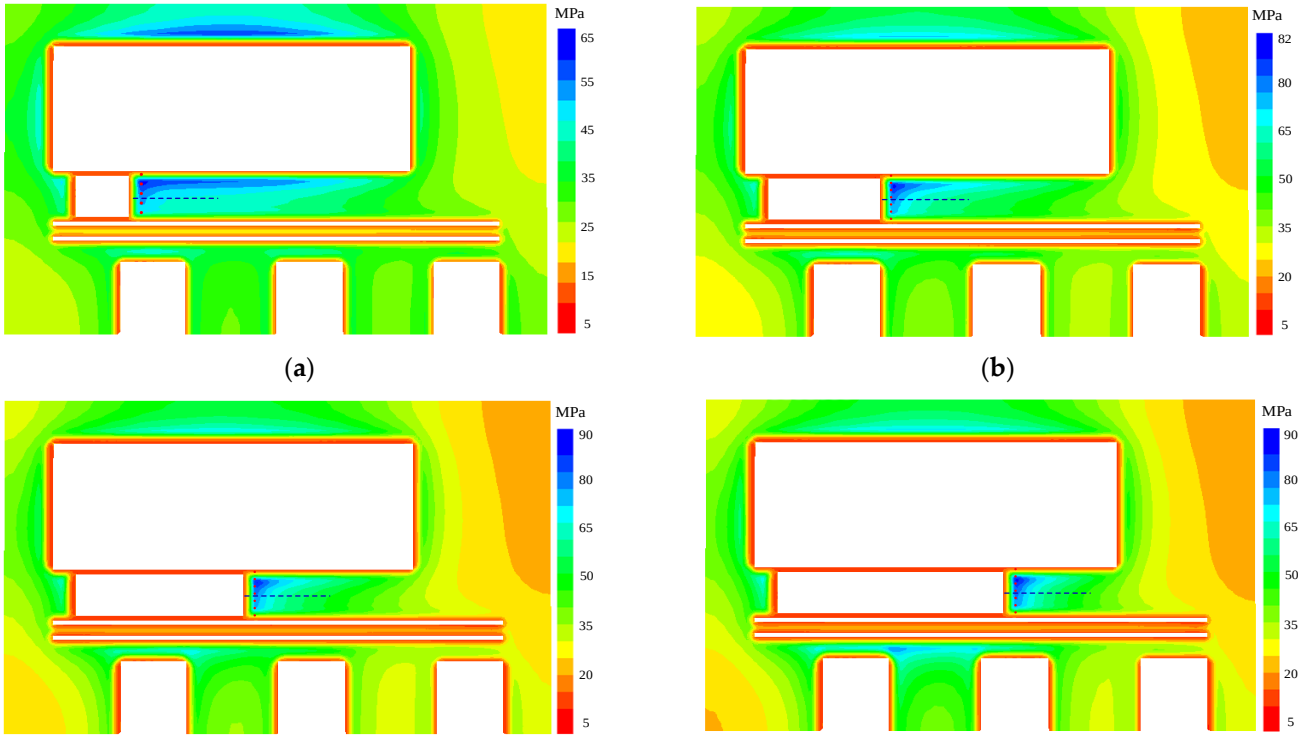

Figure 8. Cloud diagram of coal rock mass stress distribution during mining of 6304 working face. (**a**) 50 m. (**b**) 100 m. (**c**) 150 m. (**d**) 200 m.

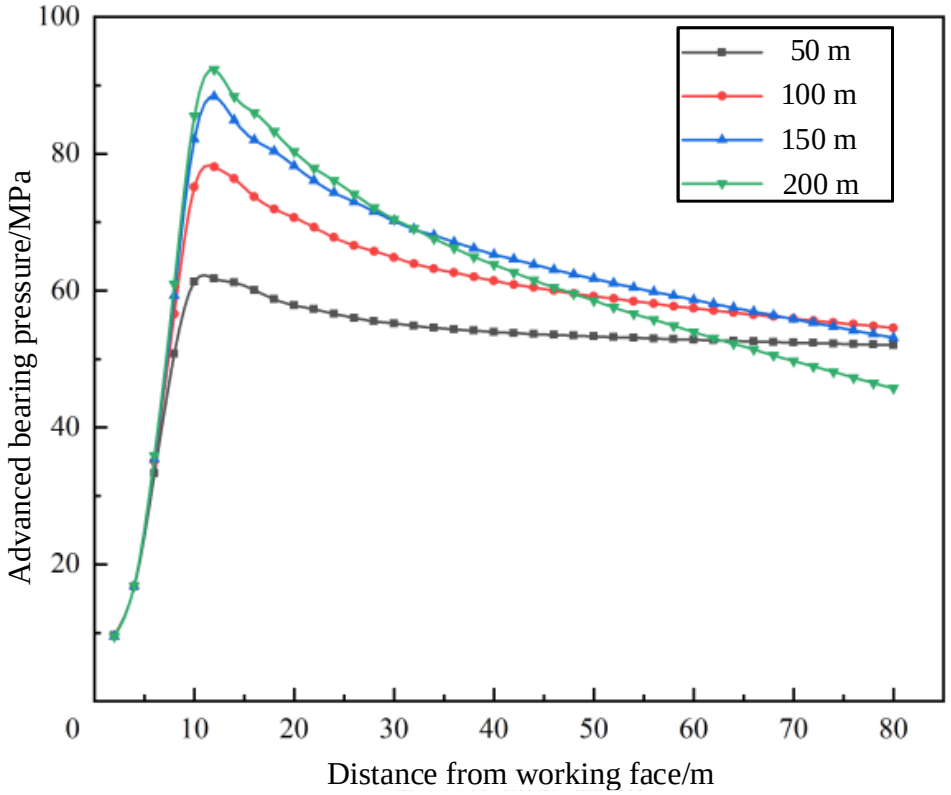

Figure 9. Advanced bearing pressure curve of 6304 working face.

Figure 10 shows the stress distribution diagram along the inclination of the working face in front of the coal wall under different advancing steps (measuring line is shown by the blue dashed line in Figure 8). According to Figure 10, the coal rock mass is in a high-stress state (between 35 and 45 MPa) during the mining period; this is due to the superposition of deep high stress, lateral bearing pressure of the goaf, and advanced bearing pressure of 6304 working face. The stress above the working face is much greater than that of the original rock (16.6 MPa). It is easier to make the coal mass achieve the limit equilibrium state of overall instability in this situation.

3.2. Energy Analysis of Hard Roof Breaking

With the progress of mining, the exposed length and area of the hard roof increases continuously. When the hard roof reaches its maximum span, it will initiate the fracture. Rock bust accidents are easily caused by the release of accumulated elastic energy into the mining area once the roof is broken.

The mechanical model of the hard roof is established using the thin plate theory in conjunction with the working conditions of a narrow coal pillar working face. Before roof collapse, the supporting side of the coal pillar adjacent to the goaf (two roadways) is considered as a simple supporting edge, and the coal seam in front of the working face is considered as a fixed supporting edge (Figure 11). In the figure, the upper, lower, and left boundaries are simple supporting edges and the right boundary is a fixed supporting edge. It is assumed that the overlying load is uniform load q; the x direction is the advancing direction of the working face; a is the hard roof breaking step of the working face; the y direction is the working face layout direction; and b is the width of the working face.

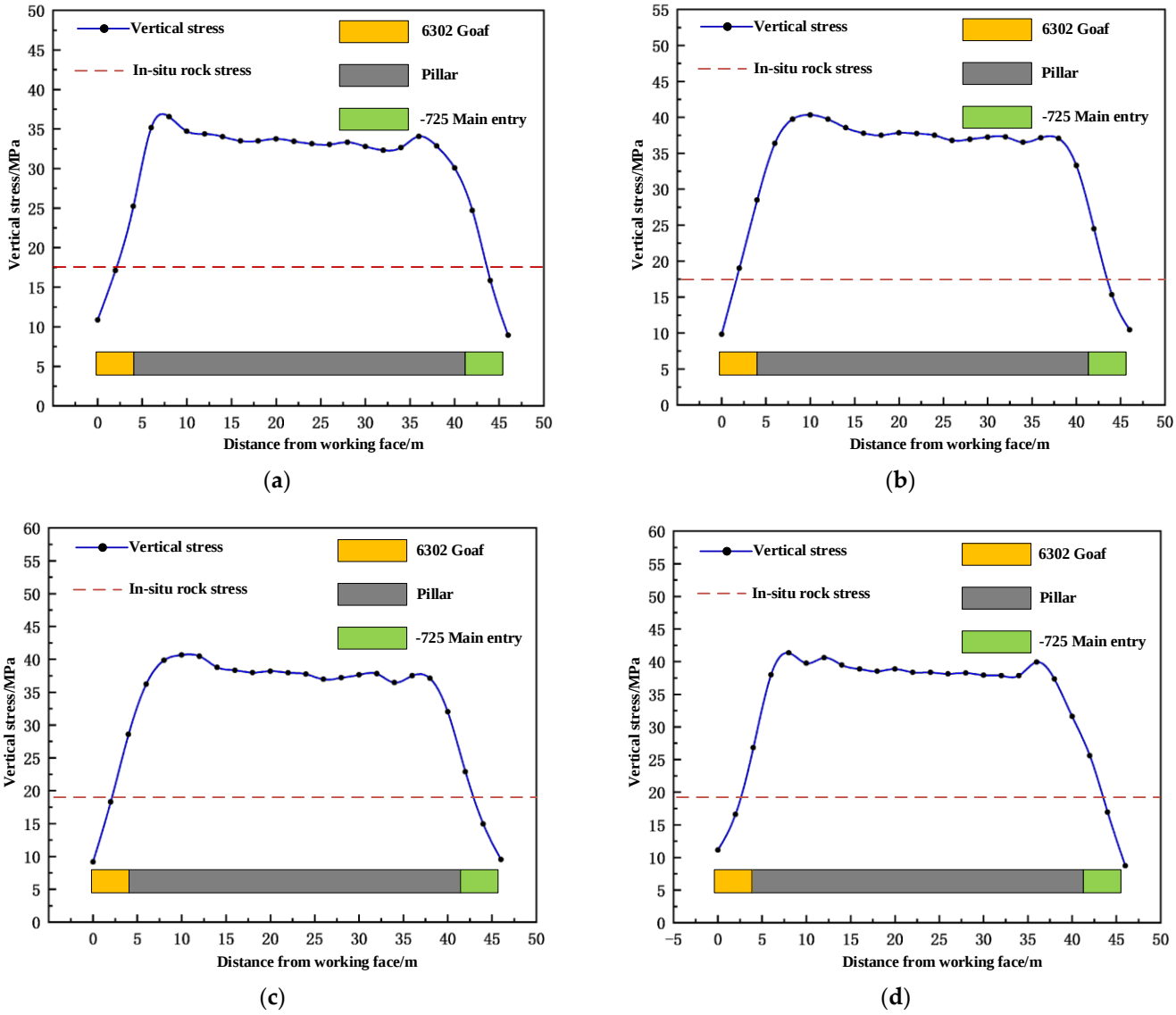

Figure 10. Schematic diagram of stress distribution ahead of working face at different advancing steps (along the inclination of working face). (**a**) 50 m. (**b**) 100 m. (**c**) 150 m. (**d**) 200 m.

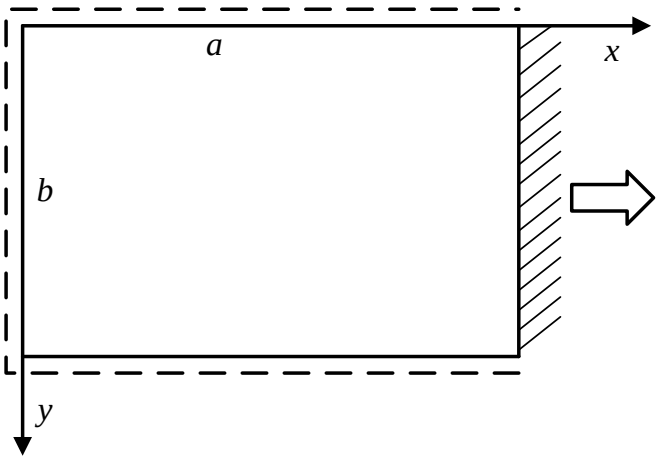

Figure 11. Hard roof breaking model.

According to the elastic thin plate theory, the roof bending strain energy can be obtained through the following expression:

$$U_w = \frac{D}{2}\iint\left\{(\nabla^2 w)^2 - 2(1-\mu)\left[\frac{\partial^2 w}{\partial x^2}\frac{\partial^2 w}{\partial y^2} - (\frac{\partial^2 w}{\partial x \partial y})^2\right]\right\}dxdy \quad (1)$$

$$D = Eh^3/12\left(1-\mu^2\right) \quad (2)$$

where, U_w is the roof bending strain energy, KJ; D is the bending stiffness, N/m; ∇^2 is Laplace operator; w is deflection, mm; E is the elastic modulus of rock, MPa; h is thickness of rock, m; μ is Poisson's ratio of rock.

According to the Rayleigh-Ritz method, the total potential energy is expressed as:

$$I = U_w - \iint qwdxdy \quad (3)$$

It can be seen from elastic mechanics that the deflection expression should satisfy the following displacement boundary conditions: when $y = 0$ or b, w is 0; when $x = 0$ or a, w is 0; when $x = a$, the first derivative of w is equal to 0. The deflection expression satisfying the boundary conditions is set as:

$$w = Ax(x-a)^2\sin(\frac{\pi}{b}y) \quad (4)$$

where, A is coefficient of deflection expression.

Substituting Equation (4) into Equation (3) and setting $\partial I/\partial A = 0$, it can be obtained that:

$$A = \frac{35a^4b^4q}{\pi D(420a^3b^4 + \pi^4a^7 + 28\pi^2a^5b^2)} \quad (5)$$

Substituting Equations (2) and (5) into Equation (1), the roof bending strain energy can be obtained as follows:

$$U_w = \frac{35a^8b^5q^2(1-\mu^2)}{\pi^2Eh^3(420a^3b^4 + \pi^4a^7 + 28\pi^2a^5b^2)} \quad (6)$$

The accumulated elastic strain energy of the roof is calculated based on the actual geological conditions of the working face. The parameters are as follows: the average mining depth of the working face is 750 m; the overlying load is 16.6 MPa; the hard rock stratum above coal seam has a thickness of 15.2 m, with the elastic modulus of 38 GPa, and Poisson's ratio of 0.22. Based on this, the accumulated energy of the hard roof is calculated as 79.9×10^6 J. Once the hard roof breaks, the energy that is theoretically released will reach levels high enough to cause a rock burst.

3.3. Rock Burst inducing Mechanism of Narrow Coal Pillar Working Face

During roadway excavation, the direction of maximum horizontal principal stress is approximately perpendicular to the direction of roadway excavation, which has an important influence on roadway stability. Meanwhile, the excavated roadway is located in the influence range of the peak lateral bearing pressure of the goaf, and the two roadways are under greater pressure during the excavation, providing the static load condition for the occurrence of rock bursts.

During the mining process, a high-stress concentration exists in the narrow coal pillar working face due to the influence of the large burial depth, lateral bearing pressure of adjacent goaf, and advanced bearing pressure of this working face, providing static load condition for the occurrence of rock burst. The movement space of the overlying rock stratum above the coal seam is enlarged as mining progresses in this working face, and the movement and breakage of the overlying rock stratum provide dynamic load conditions for

the occurrence of rock burst. The narrow coal pillar eventually tends to approach the critical destabilization stage under the influence of substantial static stress. When it is subjected to dynamic load (energy released instantaneously when the overlying rock stratum breaks), it is extremely easy to reach the critical condition for the occurrence of rock burst, ultimately leading to a rock burst accident (as shown in Figure 12).

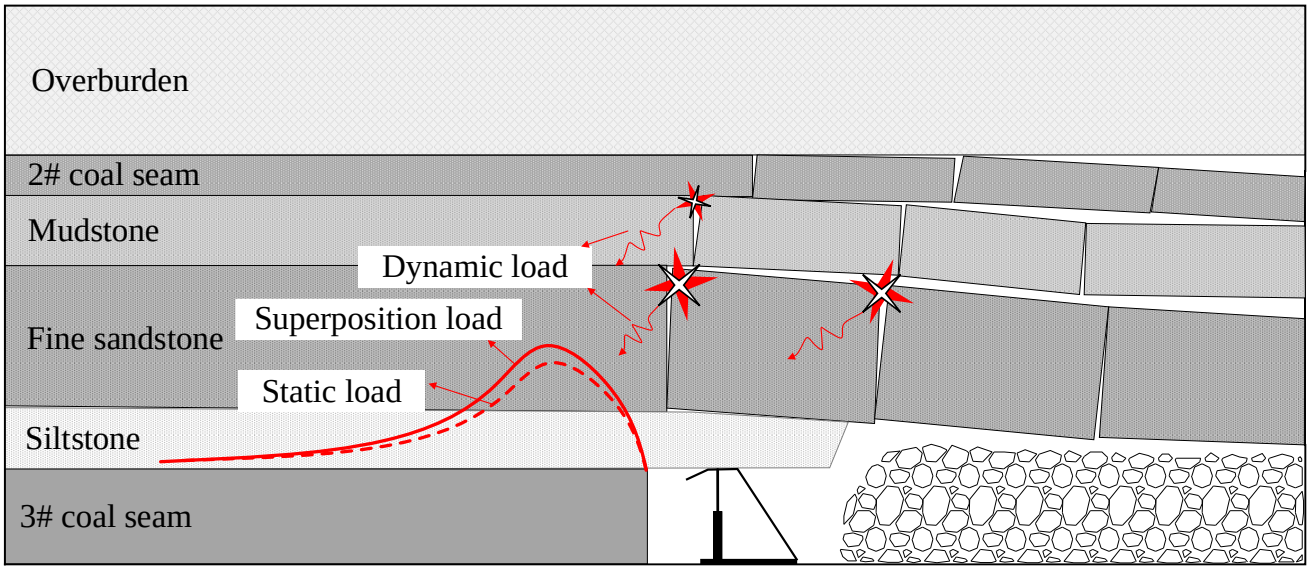

Figure 12. Schematic diagram of rock burst induced by dynamic load and static load superposition.

4. Prevention and Control of Rock Burst of Narrow Coal Pillar Working Face

4.1. Prevention and Control Measures against Rock Burst

Based on the rock burst-inducing mechanism for mining in narrow coal pillar working face under complex conditions, the main sources of rock burst initiation are high-stress superposition of near-field coal seam and dynamic load caused by far-field roof breaking. Therefore, it is necessary to perform rock burst prevention and control on the basis of reducing stress concentration on coal seam and dynamic load disturbance caused by roof breaking [29]. A coordinated control scheme, which focuses on strong pressure relief and strong support in near-field high-pressure coal mass and pressure relief in far-field high-level hard roof with an advanced pre-cracking roof, is formulated.

4.1.1. Coordinated Control of Strong Pressure Relief and Strong Support for Near-Field High-Pressure Coal Mass

During roadway excavation, large diameter boreholes in coal seams are drilled in the excavated head face and the solid coal side to reduce the stress concentration of coal seam. The diameter and depth of the borehole are 150 mm and 20 m, respectively, and the height from the borehole to the coal seam floor is 1.2 m. Two boreholes are arranged at the excavated head face, and the borehole spacing on solid coal sides is 3 m, as shown in Figure 13a. On the basis of borehole drilling during excavation, large diameter boreholes are drilled during mining in the working face to release pressure on the sides of solid coal, and the borehole spacing for pressure relief of the coal side is 3.0 m, as shown in Figure 13b.

Considering that high-strength pressure relief may destroy the original support system, bolts with a torque not less than 300 N·m and a length of 2.4 m are used for roadway support during excavation. The roof and solid coal side are supported by anchor cable with a tensile strength of 290–480 kN and a length of 7.5 m, as shown in Figure 14. To further increase the ability of roadways to withstand high-energy events, the support is strengthened by using a single pillar somewhere around 40 m behind the excavated face.

Through monitoring and analysis during excavation and mining, as the countermeasures of strong support and strong pressure relief are adopted during excavation and

mining in the 6304 working face, the roof separation is effectively controlled and the deformation of surrounding rock is restrained. The support effect is shown in Figure 15.

4.1.2. Pressure Relief in the Far-Field High-Level Hard Roof with Advanced Pre-Cracking Roof

To avoid the large energy event caused by the roof movement during mining, the pressure relief in the far-field hard roof with an advanced pre-cracking roof is decompressed at the open-off cut and the two roadways before mining. In this study, blasting method is adopted to break the hard roof. Based on the overlying rock stratum structure, the blasting borehole parameters are designed as follows: the borehole diameter = 75 mm, borehole length = 25 m, powder charge length = 14 m (red line in Figure 16), sealing length = 11 m (blue line in Figure 16), inclination angle = 80°, and blasting borehole spacing = 10 m, as shown in Figure 16.

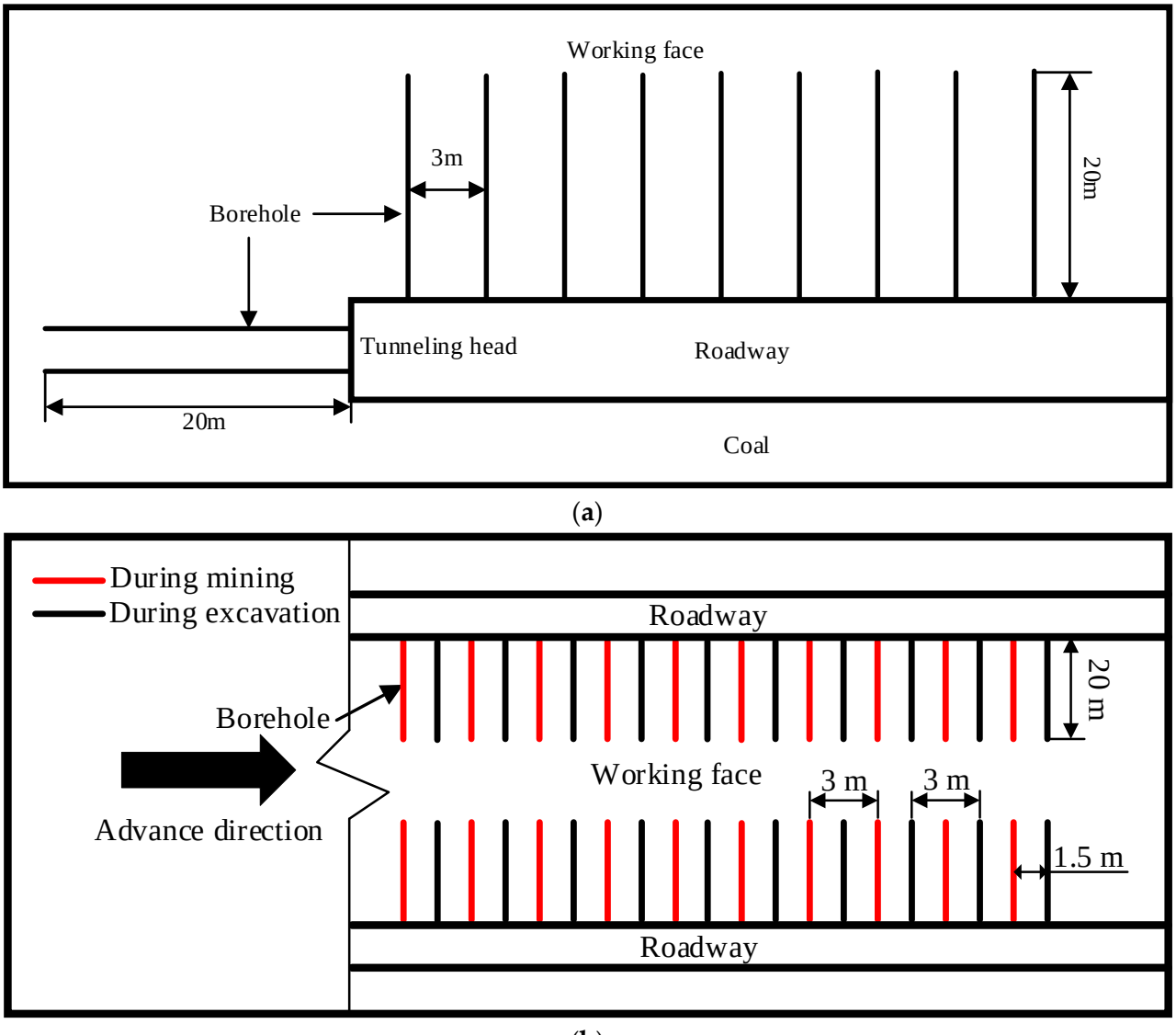

Figure 13. Arrangement drawing of large-diameter pressure relief borehole during excavation and mining. (**a**) Arrangement drawing of large-diameter pressure relief boreholes during excavation. (**b**) Arrangement drawing of large-diameter pressure relief boreholes during mining.

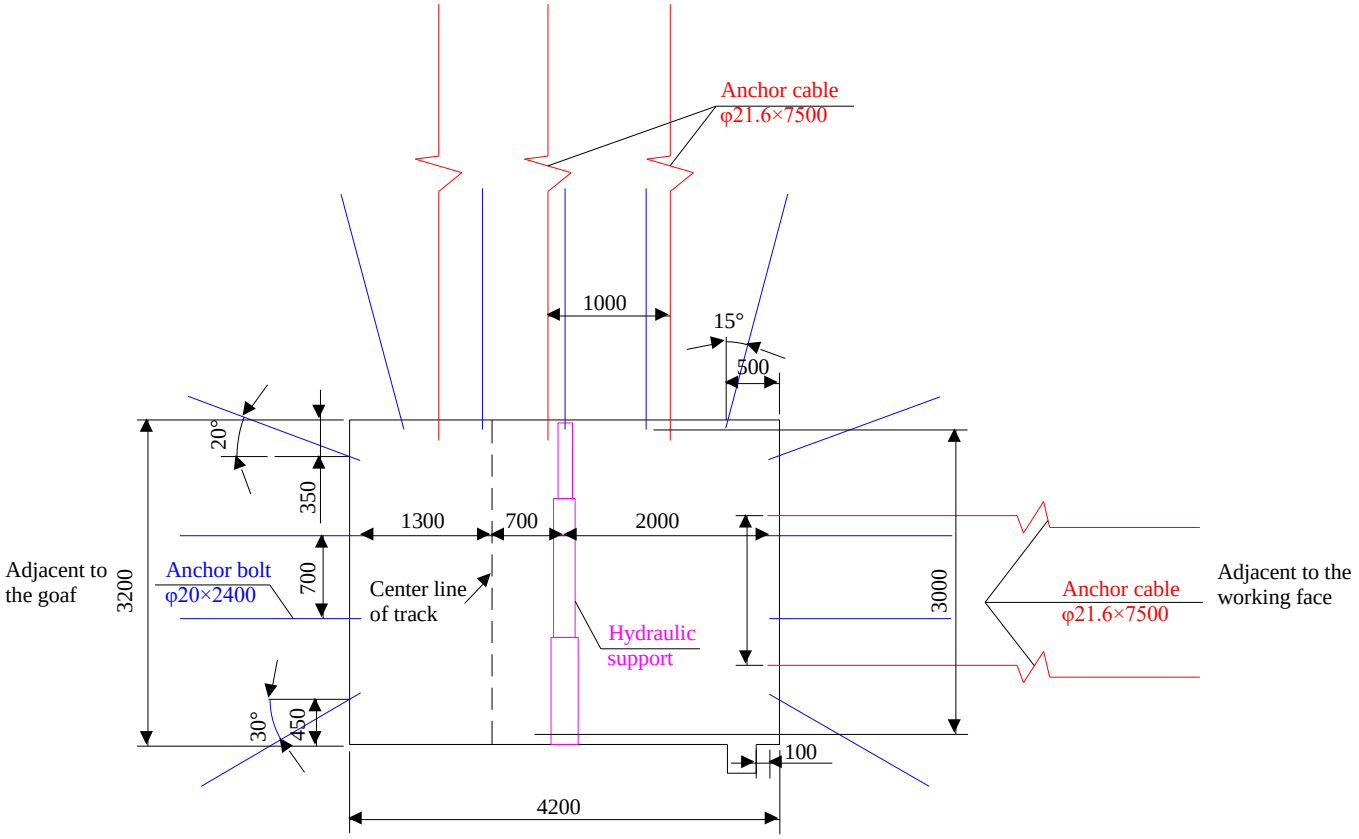

Figure 14. Schematic diagram of the roadway support scheme (unit: mm).

Figure 15. Support effect of the roadway.

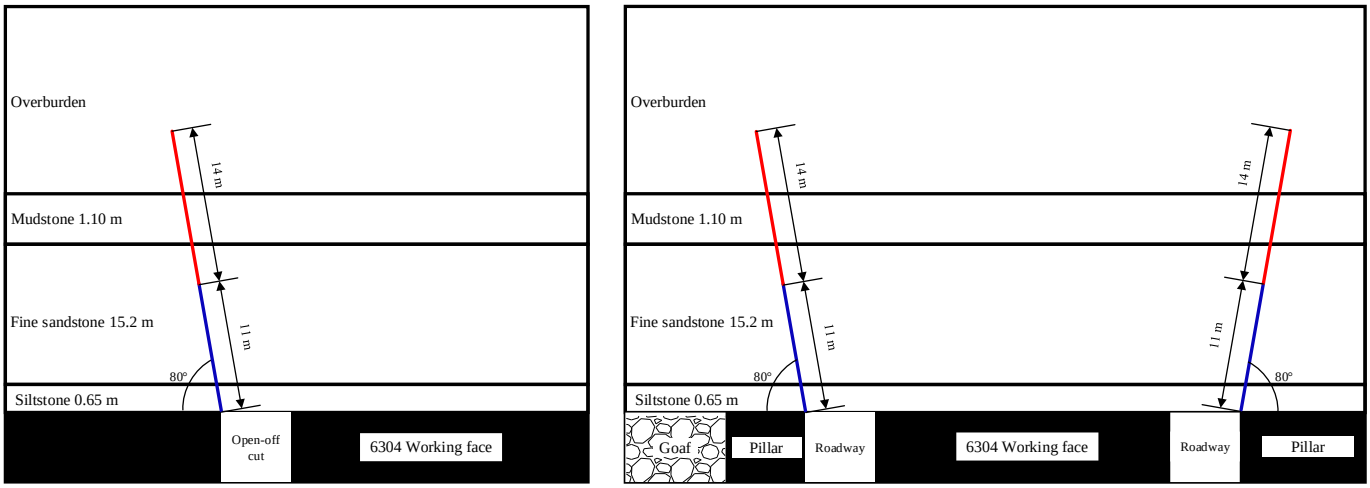

Figure 16. Schematic diagram of roof breaking scheme. (**a**) Near the open-off cut. (**b**) Near the two roadways.

4.2. Evaluation of Pressure Relief Effect

After pressure relief by blasting (hard roof) and large diameter borehole (coal seam), the seismic wave computed tomography-derived method and microseismic monitoring are used to verify the pressure relief effect. Herein, the seismic wave computed tomography-derived technology is used to image the velocity of the wave propagating in coal rock mass in the form of a stress nephogram in the corresponding area by means of computer. Based on the timing and distance of seismic sources received by stations, seismic source wave velocity is inverted. Based on the principle that wave velocity is positively correlated with stress in coal rock mass, the stress distribution in coal rock mass can be determined [30–34].

(1) Seismic wave computed tomography-derived

The first seismic wave computed tomography-derived on the working face is carried out before mining, as shown in Figure 17, and high-stress areas (areas A and B) are obtained. After the pressure relief, a second seismic wave computed tomography-derived is performed, as shown in Figure 18. It should be noted that the seismic wave was not received in area B. In comparison to Figures 17 and 18, the high-stress zone of the coal seam changes following pressure relief, and the stress level of the coal seam in the original high-stress zone is significantly reduced (area A).

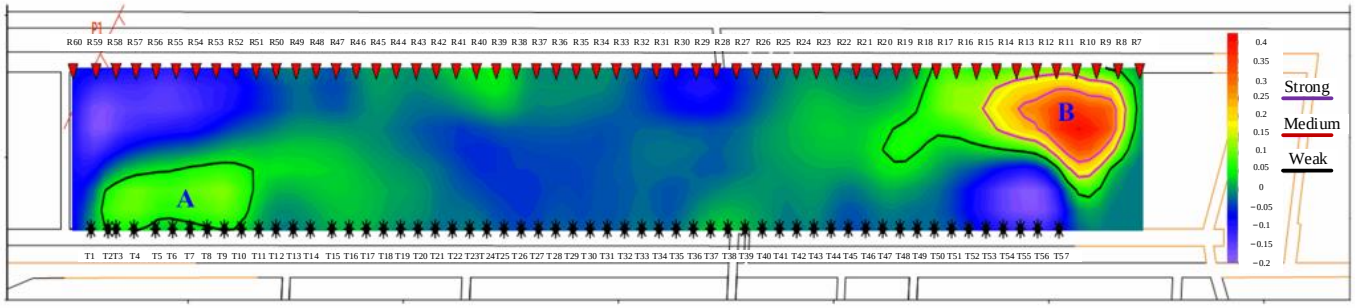

Figure 17. Coal rock stress distribution diagram of 6304 working face (the first computed tomography-derived detection results).

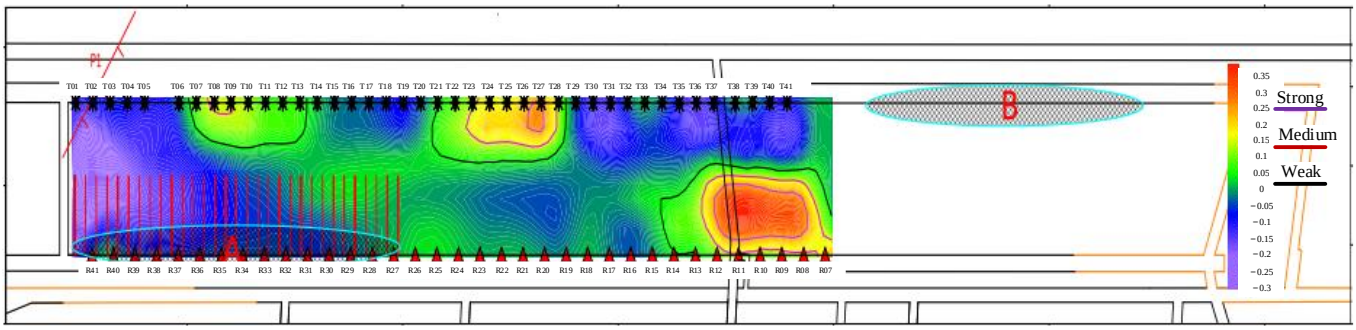

Figure 18. Coal rock stress distribution diagram of 6304 working face (computed tomography-derived detection results after pressure relief).

(2) Microseismic monitoring

The energy events occurring during mining are collected through the arranged microseismic monitoring points. The maximum daily energy value of microseismic monitoring within 25 days before and after the pressure relief is used as the test data for the pressure relief effect, as shown in Figure 19. In the figure, the blue line represents the weak burst risk warning line and the yellow line represents the medium burst risk warning line. It can be seen from the figure that the values for the maximum daily energy observed by microseismic monitoring within 20 days before pressure relief are mostly above 5×10^4 J, two of which reach 1×10^5 J, and three of which are close to 1×10^5 J. After pressure relief, the overall energy values monitored by the microseismic system are significantly reduced, most of which are below 2.5×10^4 J, and no events with the energy value exceeding 1×10^5 J occur. The maximum energy value is relatively low, and the maximum energy is significantly reduced compared with that before advanced pre-cracking roof.

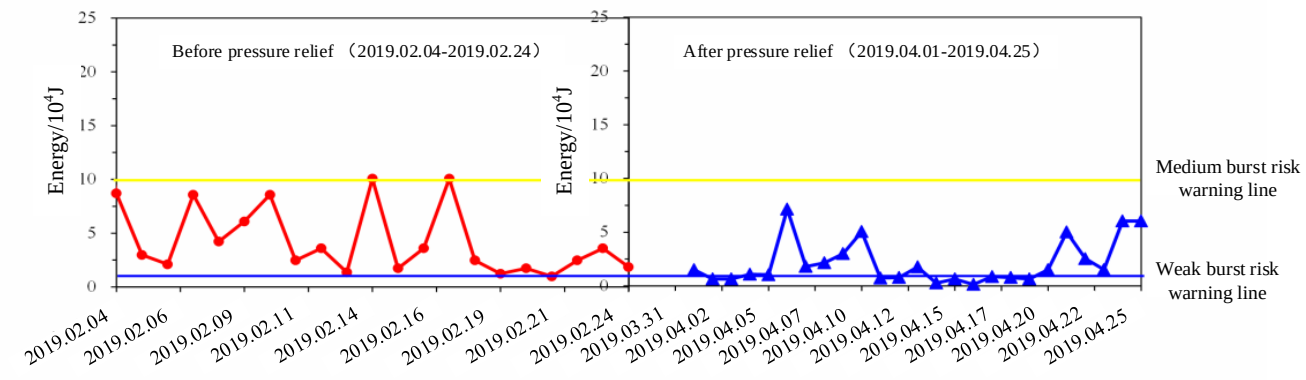

Figure 19. Daily maximum energy curve within 25 days before and after blasting.

5. Conclusions

(1) During roadway excavation, the two roadways of 6304 working face are located within the influenced range of 6302, 8301, 8302, and 8303 goafs, which provides the static load condition for the occurrence of rock burst. Influenced by the peak lateral bearing pressure of adjacent goafs and maximum horizontal principal stress (perpendicular to roadway tunnelling direction), it is difficult to ensure roadway stability.

(2) During mining, the narrow coal pillar working face experiences high static load (crustal stress, lateral bearing pressure of surrounding goafs, and advanced bearing pressure of working face). Meanwhile, movement and breakage of overlying rock stratum on coal seam provide dynamic load conditions (energy releases instantaneously when the overlying rock stratum breaks) for the occurrence of rock burst. Once the hard roof breaks, the energy that is theoretically released will reach 79.9×10^6 J. Under the superposition of "near-field high static load + far-field dynamic load", the

critical destabilization value in narrow coal pillar working face can easily be exceeded, ultimately leading to a rock burst accident.

(3) A coordinated control scheme, which focuses on strong pressure relief and strong support in near-field high-pressure coal mass and pressure relief in far-field high-level hard roof with an advanced pre-cracking roof, is formulated. The field monitoring results show that the overall energy values monitored by the microseismic system are significantly reduced and most of which are below 2.5×10^4 J after pressure relief. It provides a beneficial reference for the prevention and control practice of rock burst at the narrow working face under similar conditions.

Author Contributions: Conceptualization, W.L. and B.J; methodology, S.G.; software, H.C.; validation, H.C.; formal analysis, X.C. and H.C.; investigation, S.G. and W.L.; data curation, X.C.; writing—original draft preparation, H.C. and W.L.; writing—review and editing, S.G. and B.J.; visualization, X.C.; project administration, S.G.; funding acquisition, B.J. All authors have read and agreed to the published version of the manuscript.

Funding: This research is funded by the National Natural Science Foundation of China (52004144).

Institutional Review Board Statement: Not Applicable.

Informed Consent Statement: Not Applicable.

Data Availability Statement: The data used to support the finding of this study are available from the corresponding author upon request.

Acknowledgments: This research is supported by the National Natural Science Foundation of China (52004144) and the support is gratefully acknowledged.

Conflicts of Interest: The authors declare that they have no conflicts of interest regarding the publication of this work.

References

1. Liu, F.; Cao, W.J.; Zhang, J.M.; Cao, G.M.; Guo, L.F. Current technological innovation and development direction of the 14th Five-Year Plan period in China coal industry. *J. China Coal Soc.* **2021**, *46*, 1–15.
2. Wang, G.F.; Reng, S.H.; Pang, Y.H.; Qu, S.J.; Zheng, D.Z. Development achievements of China's coal industry during the 13th Five-Year Plan period and implementation path of "dual carbon" target. *J. China Coal Soc.* **2021**, *49*, 1–10.
3. Xie, H.P.; Reng, S.H.; Xie, Y.C.; Jiao, X.M. Development opportunities of the coal industry towards the goal of carbon neutrality. *J. China Coal Soc.* **2021**, *46*, 2197–2211.
4. Cao, A.Y.; Chen, F.; Liu, Y.Q.; Dou, L.M.; Wang, C.B.; Yang, X.; Bai, X.Q.; Song, S.K. Response characteristics of rupture mechanism and source arameters of mining tremors in frequent coal burst area. *J. China Coal Soc.* **2022**, *47*, 722–733.
5. Pan, J.F.; Liu, S.H.; Gao, J.M.; Sun, X.K.; Xia, Y.X.; Wang, Q. Prevention theory and technology of rock burst with distinguish dynamic and static load sources in deep mine roadway. *J. China Coal Soc.* **2020**, *45*, 1607–1613.
6. Wang, E.Y.; Feng, J.J.; Zhang, Q.M.; Kong, X.G.; Liu, X.F. Mechanism of rockburst under stress wave in mining spac. *J. China Coal Soc.* **2020**, *45*, 100–110.
7. Dou, L.M.; Lu, C.P.; Mou, Z.L.; Qin, Y.H.; Yao, J.M. Intensity weakening theory for rockburst and its application. *J. China Coal Soc.* **2005**, *30*, 690–694.
8. Zhao, Y.X.; Zhou, J.L.; Liu, W.G. Characteristics of ground pressure and mechanism of coal burst in the gob side roadway at Xinjie deep mining area. *J. China Coal Soc.* **2020**, *45*, 1595–1606.
9. Zhao, T.-B.; Guo, W.-Y.; Tan, Y.-L.; Yin, Y.-C.; Cai, L.-S.; Pan, J.-F. Case Studies of Rock Bursts Under Complicated Geological Conditions During Multi-seam Mining at a Depth of 800 m. *Rock Mech. Rock Eng.* **2018**, *51*, 1539–1564. [CrossRef]
10. Zhou, K.; Dou, L.; Gong, S.; Li, J.; Cao, J. Study of Rock Burst Risk Evolution in Front of Deep Longwall Panel Based on Passive Seismic Velocity Tomography. *Geofluids* **2020**, *2020*, 8888413. [CrossRef]
11. Wang, J.-C.; Jiang, F.-X.; Meng, X.-J.; Wang, X.-Y.; Zhu, S.-T.; Feng, Y. Mechanism of Rock Burst Occurrence in Specially Thick Coal Seam with Rock Parting. *Rock Mech. Rock Eng.* **2016**, *49*, 1953–1965. [CrossRef]
12. Keneti, A.; Sainsbury, B.-A. Review of published rockburst events and their contributing factors. *Eng. Geol.* **2018**, *246*, 361–373. [CrossRef]
13. Yang, Y.; Wei, S.; Li, K. Inverse analysis of dynamic failure characteristics of roadway surrounding rock under rock burst. *Energy Sci. Eng.* **2021**, *9*, 2298–2310. [CrossRef]
14. Xu, L.; Lu, K.; Pan, Y.; Qin, Z. Study on rock burst characteristics of coal mine roadway in China. *Energy Sources Part A Recovery Util. Environ. Eff.* **2022**, *44*, 3016–3035. [CrossRef]

15. Zhao, T.-B.; Guo, W.-Y.; Tan, Y.-L.; Lu, C.-P.; Wang, C.-W. Case histories of rock bursts under complicated geological conditions. *Bull. Eng. Geol. Environ.* **2018**, *77*, 1529–1545. [CrossRef]
16. Zhou, N.; Liu, H.F.; Zhang, J.X.; Yan, H. Study on Rock Burst Event Disaster and Prevention Mechanisms of Hard Roof. *Adv. Civ. Eng.* **2019**, *2019*, 6910139. [CrossRef]
17. Lu, A.; Dou, L.; Bai, J.; Chai, Y.; Zhou, K.; Kan, J.; Cao, J.; Song, S.; Deyuan, F. Mechanism of Hard-Roof Rock Burst Control by the Deep-Hole Blasting: Numerical Study Based on Particle Flow. *Shock Vib.* **2021**, *2021*, 9527956. [CrossRef]
18. Shi, X.; Zhang, X.; Jiang, F.; Wang, H.; Wei, J. Study on Practice of Rockburst Accident Prevention in Multi-Seam Mining Controlled by Large Fault and Hard Roof. *Geotech. Geol. Eng.* **2020**, *38*, 6843–6853. [CrossRef]
19. Guo, W.; Li, Y.; Yin, D.; Zhang, S.; Sun, X. Mechanisms of rock burst in hard and thick upper strata and rock-burst controlling technology. *Arab. J. Geosci.* **2016**, *9*, 561. [CrossRef]
20. Wang, C.; Cao, A.; Zhu, G.; Jing, G.; Li, J.; Chen, T. Mechanism of rock burst induced by fault slip in an island coal panel and hazard assessment using seismic tomography: A case study from Xuzhuang colliery, Xuzhou, China. *Geosci. J.* **2017**, *21*, 469–481. [CrossRef]
21. Khademian, Z.; Ugur, O. Computational framework for simulating rock burst in shear and compression. *Int. J. Rock Mech. Min. Sci.* **2018**, *110*, 279–290. [CrossRef]
22. Lu, C.-P.; Liu, B.; Liu, B.; Liu, Y.; Wang, H.-Y.; Zhang, H. Anatomy of mining-induced fault slip and a triggered rockburst. *Bull. Eng. Geol. Environ.* **2019**, *78*, 5147–5160. [CrossRef]
23. Manouchehrian, A.; Cai, M. Numerical modeling of rockburst near fault zones in deep tunnels. *Tunn. Undergr. Space Technol.* **2018**, *80*, 164–180. [CrossRef]
24. Wang, P.; Jiang, L.-S.; Zheng, P.-Q.; Qin, G.-P.; Zhang, C. Inducing mode analysis of rock burst in fault-affected zone with a hard–thick stratum occurrence. *Environ. Earth Sci.* **2019**, *78*, 467. [CrossRef]
25. Jiang, F.X.; Cheng, G.; Feng, Y.; Wang, C.W.; Xu, Y.Y. Research on coal overall instability of isolated working face with irregular gobs on both sides. *Chin. J. Geotech. Eng.* **2015**, *34* (Suppl. S2), 4164–4170.
26. Xue, C.C.; Cao, A.Y.; Niu, F.W.; Wang, X.Y.; Shen, Z.P.; Tang, K. Mechanism and prevention of rock burst in deep irregular isolated coal pillar. *Chin. J. Geotech. Eng.* **2021**, *38*, 479–486.
27. Du, T.T.; Ju, W.J.; Chen, J.Q.; Zhang, C.J.; Li, H.P.; Sun, R.D. Mechanism of rock burst in fully mechanized caving faces under residual coal seams with hard roof. *Chin. J. Geotech. Eng.* **2021**, *38*, 1144–1151.
28. Zhu, G.A.; Dou, L.M.; Ding, Z.W.; Xie, J.H. Pre-evaluation for rock burst risks in island longwall panel before mining. *Chin. J. Geotech. Eng.* **2018**, *40*, 819–827.
29. Tan, Y.L.; Guo, W.Y.; Zhao, T.B.; Meng, X.J. Coal rib burst mechanism in deep roadway and "stress relief—Support reinforcement" synergetic control and prevention. *J. China Coal Soc.* **2020**, *45*, 66–81.
30. Cao, A.; Dou, L.; Cai, W.; Gong, S.; Liu, S.; Jing, G. Case study of seismic hazard assessment in underground coal mining using passive tomography. *Int. J. Rock Mech. Min. Sci.* **2015**, *78*, 1–9. [CrossRef]
31. Gao, M.; Zhao, H.; Zhao, Y.; Gao, X.; Wang, X. Investigation on the Vibration Effect of Shock Wave in Rock Burst by In Situ Microseismic Monitoring. *Shock Vib.* **2018**, *2018*, 8517806. [CrossRef]
32. Li, Y.; Zhou, C.; Lian, H. Rockburst Inducement Mechanism and Its Prediction Based on Microseismic Monitoring. *Geofluids* **2021**, *2021*, 4028872. [CrossRef]
33. Ma, T.-H.; Tang, C.-A.; Liu, F.; Zhang, S.-C.; Feng, Z.-Q. Microseismic monitoring, analysis and early warning of rockburst. *Geomat. Nat. Hazards Risk* **2021**, *12*, 2956–2983. [CrossRef]
34. Yu, Q.; Zhao, D.; Xia, Y.; Jin, S.; Zheng, J.; Meng, Q.; Mu, C.; Zhao, J. Multivariate Early Warning Method for Rockburst Monitoring Based on Microseismic Activity Characteristics. *Front. Earth Sci.* **2022**, *10*, 837333. [CrossRef]